## The VP16 Activation Domain Establishes an Active Mediator Lacking CDK8 in Vivo\*S

Received for publication, September 1, 2006, and in revised form, November 1, 2006 Published, JBC Papers in Press, November 29, 2006, DOI 10.1074/jbc.M608451200

Thomas Uhlmann<sup>1</sup>, Stefan Boeing<sup>1</sup>, Michael Lehmbacher, and Michael Meisterernst<sup>2</sup>

From the Gene Expression, National Research Center for Environment and Health, Marchionini-Strasse 25, D-81377 Munich, Germany

VP16 has been widely used to unravel the mechanisms underlying gene transcription. Much of the previous work has been conducted in reconstituted in vitro systems. Here we study the formation of transcription complexes at stable reporters under the control of an inducible Tet-VP16 activator in living cells. In this simplified model for gene activation VP16 recruits the general factors and the cofactors Mediator, GCN5, CBP, and PC4, within minutes to the promoter region. Activation is accompanied by only minor changes in histone acetylation and H3K4 methylation but induces a marked promoter-specific increase in H3K79 methylation. Mediated through contacts with VP16 several subunits of the cleavage and polyadenylation factor (CPSF/ CstF) are concentrated at the promoter region. We provide in vitro and in vivo evidence that VP16 activates transcription through a specific MED25-associated Mediator, which is deficient in CDK8.

The herpes simplex virus-encoded protein VP16 is a potent activator that controls the transcription of immediate early viral genes through the interaction with host cell factors (1). VP16 harbors a strong activation domain that functions well in both yeast and human cells when tethered to independent DNA-binding domains (2-4). Based on these properties, fusion proteins of VP16 with GAL4 or DNA-binding domains of other transactivators have been widely used as models to investigate the basic principles of transcription activation.

In conjunction with molecular interactions involving the general transcription factors TFIIA, TBP, TFIIB, and the TBPassociated factors (5-9), VP16 increases the number of functional pre-initiation complexes in vitro. Furthermore, VP16 stimulates open complex formation, which relates to interactions with the p62 subunit of TFIIH and the general cofactor PC4 (10).

Comparative binding studies and functional experiments pointed to a key role for the cofactors CBP, STAGA/TFTC, and Mediator (11-16) in activation by VP16 (17). CBP interacts specifically with the C-terminal (H2) region of VP16, whereas Mediator binds tightly to both the N-terminal (H1) and C-terminal (H2) regions of the activation domain (18, 19). The histone acetyltransferase activity of CBP (p300) is critical for activation by VP16 in chromatin (20, 21). The other major histone acetyltransferase, GCN5, which is part of the SAGA-STAGA/ TFTC complex, is also recognized by VP16 (17, 22, 23). Further related to chromatin accessibility, the remodeling Swi/Snf complex interacts with VP16 (24).

VP16 binds Mediator tightly and specifically through the MED17 and the MED25 subunits (19, 25). Overexpression of the MED25 Mediator-binding domain has a dominant negative effect on VP16 activation, which substantiates the critical influence of a MED25-associated Mediator (19). Furthermore, Mediator apparently functions synergistically with other target proteins such as the histone acetyltransferases, CBP and GCN5, that are also necessary for activation by VP16 in living cells (17).

Here, we use an inducible Tet-VP16 in combination with stable reporter plasmids in HeLa cells and conducted a comprehensive molecular in vivo analysis of VP16 transcription activation. Chromatin immunoprecipitation (ChIP) studies revealed the binding of many of the previously identified targets of VP16, among them GTFs, Mediator, CBP, GCN5, and PC4. We describe, for the first time, that VP16 binds to and recruits cleavage and polyadenylation factor (CPSF/CstF) to regulatory regions in vivo. Also novel, we observed in the chromatin a marked influence of VP16 on dimethylation of lysine 79 in histone H3. The ChIP and biochemical analyses point to the use of a specific active Mediator by VP16, carrying MED25 and lacking the CDK8 module. Solid-phase assays further support the notion that Mediator composition is dynamically affected on genes, in an ATP-dependent manner. This apparently leads to the establishment of a variant Mediator enriched in core subunits and MED25 and lacking CDK8.

#### **EXPERIMENTAL PROCEDURES**

Plasmid Construction—Plasmid pTU10 contains the EBV origin, an EBNA1 expression cassette, the hygromycin resistance gene as a genetic selection marker, and the luciferase gene under the control of a Tet-operator (tetO) linked to the V $\beta$ 12-3



<sup>\*</sup> This work was supported by the Deutsche Forschungsgemeinschaft (Grants SFB/TR5 and SFB646), the STREP program of the European Union (Grant HPRN-CT-2002-00261), and the Bundesministerium für Bildung und Forschung programs (Grants 0313030A and 0313427) (to M. M.). The costs of publication of this article were defrayed in part by the payment of page charges. This article must therefore be hereby marked "advertisement" in accordance with 18 U.S.C. Section 1734 solely to indicate this fact.

The on-line version of this article (available at http://www.jbc.org) contains supplemental Figs. S1 and S2.

<sup>&</sup>lt;sup>1</sup> Both authors contributed equally to this work.

<sup>&</sup>lt;sup>2</sup> To whom correspondence should be addressed. Tel.: 49-89-709-9202; Fax: 49-89-709-9537; E-mail: Meisterernst@gsf.de.

<sup>&</sup>lt;sup>3</sup> The abbreviations used are: TF, transcription factor; ChIP, chromatin immunoprecipitation; PC4, positiver cofactor 4; CPSF/CstF, cleavage and polyadenylation stimulator factors; CBP (p300), cAMP-response element-binding protein (CREB)-binding protein; CDK8, cyclin dependent kinase 8; GTF, general transcription factor; TBP, TATA-binding protein; RNAPII, RNA polymerase II; PIC, preinitiation complex; EBV, Epstein-Barr virus; PMSF, phenylmethylsulfonyl fluoride; BSA, bovine serum albumin; GST, glutathione S-transferase; DTT, dithiothreitol; H3K79, methylation of lysine 79 of H3.

promoter. The tetO sequence comprises seven repeats of a 42-bp motif that is specifically bound by the prokaryotic tetracycline repressor. For cloning of pTU10, the V $\beta$ 12-3 wt promoter was amplified by PCR (primers VBWTP1: GGG AGA TCT TTC TCT CAG CTT TCC and VBWTP3: GGG AAG CTT CTA GAC CAG GCC CTC TG) and ligated into the BglII and HindIII sites of pGL2-basic. The promoter and the 3'-located luciferase gene were transferred into the XbaI and SalI sites of pREP4, generating plasmid pPH273. The latter was linearized with XhoI, followed by insertion of the tetO sites generated by PCR on the pTRE2 vector (Clontech), using the following primers: 5'-GCCCTTTCGTCTCGAGTTTAC-3' and 5'-TATCTCGAGCTCGACCCGGGTACC-3'. The CMV control vector (pEBNA-SVP-GL-EμCAG-rtTA, subsequently called pML53) carries an expression cassette for enhanced green fluorescence protein and the luciferase gene under the control of a bi-directional minimal CMV promoter with a central 7xtetO element in between. The CMV vector also harbors a constitutive expression cassette for the Tet repressor fused to three repeats of a minimal VP16 activation domain.

Cell Transfection and Selection—2.5  $\times$  10<sup>6</sup> HeLa Tet-On cells (Clontech) containing an integrated expression cassette for Tet-VP16 fusion protein were transfected with pTU10, or a laboratory stock of non-engineered HeLa cells were transfected with pML53, using PolyFect (Qiagen) reagent following the manufacturer's protocol. Transfected cells were selected for 2 weeks to yield stable polyclonal cells that episomally replicate pTU10 or pML53 by using 250 μg/ml hygromycin (Invitrogen) or 3 µg/ml puromycin (Sigma), respectively, until the cells resumed a normal growth rate. For their maintenance the hygromycin concentration was reduced to 125  $\mu$ g/ml and puromycin to 0.5 µg/ml. Typical copy numbers of the EBV plasmids are in the range of 1–10 in HeLa cells.

Luciferase and Transcription Assays—Cells were grown in 6-well plates and induced with 1  $\mu$ g/ml doxycycline (Sigma). 12 h after doxycycline induction, the cells were harvested and lysed in 100  $\mu$ l of Lysis buffer (Promega). The lysate was cleared by centrifugation in a table-top centrifuge. 20 µl was used for the luciferase reporter assay (Promega), another 1  $\mu$ l was used to determine the protein concentration according to Bradford (Bio-Rad). Protein concentrations were used to normalize luciferase values. In vitro transcription reactions were conducted using standard conditions and Jurkat nuclear extracts as described previously (19).

ChIP—ChIP assays were conducted mainly as described previously (26). Cells were harvested at 60 – 80% confluency and were regularly tested for luciferase induction. In detail, the following procedure was applied:  $1 \times 10^8$  HeLa cells were crosslinked by formaldehyde (Roth) at a final concentration of 1% added directly to the cell culture medium. The cross-linking reaction was allowed to proceed for 10 min at room temperature. Cross-linking was then blocked by addition of 2.5 M glycine to a final concentration of 125 mm. Cells were resuspended in 10 ml of sonification buffer (50 mm Hepes-KOH, pH 7.9, 100 mм NaCl, 1 mм EDTA, 1% Triton X-100, 0.1% deoxycholate, 1 mm PMSF), and the DNA was sheered to an average size of ~500 bp using a Branson 250-D sonifier equipped with a Microtip (duty cycle: 30% output, 15 s on, 45 s off). 0.2% Sarkosyl (Sigma) and 5.67 g of CsCl (ICN Biochemicals) were added to 10 ml of chromatin solution and centrifuged at 18 °C in an SW40 rotor at 38,000 rpm for 36-48 h. The gradient was harvested, and the collected 1-ml fractions were analyzed directly in agarose gels. Fractions containing DNA with high mobility (below a size of ~250 bp) and low mobility (containing highly cross-linked DNA-protein complexes that do not enter the gel) were omitted. CsCl fractions harboring intermediate-size fragments were pooled and dialyzed against TE (10 mm Tris-HCl, pH 8.0, 1 mm EDTA), including 5% glycerol. To remove precipitates the dialyzed sample was subjected to high speed table-top centrifugation. The sample was further pre-cleared for 2 h at 4 °C with protein G-Sepharose beads (Amersham Biosciences) equilibrated in phosphate-buffered saline with 1 mg/ml BSA (Sigma, fraction V).

For the immunoprecipitation 2  $A_{260}$  units of cross-linked DNA were incubated over night with 2–5  $\mu g$  of antibody and 2 μg of salmon sperm DNA in a final volume of 1 ml of NET buffer (55 mm Tris-HCl, pH 7.4, 150 mm NaCl, 5 mm EDTA, 0.5% Nonidet P-40). The sample was centrifuged and transferred to a new tube containing 40 µl of protein G-Sepharose or protein A-Sepharose beads equilibrated in phosphate-buffered saline containing 40  $\mu$ g of BSA and then incubated for 4 h on a rotating platform at 4 °C. Beads were washed twice with 500 μl of wash buffer I (20 mm Tris-HCl, pH 8.0, 150 mm NaCl, 2 mm EDTA, 0.1% SDS, 1% Triton X-100); twice with wash buffer II (20 mm Tris-HCl, pH 8.0, 500 mm NaCl, 2 mm EDTA, 0.1% SDS, 1% Triton X-100 (DetI) or 1% Triton X-100 (DetII)); once in wash buffer III (10 mm Tris-HCl, pH 8.0, 250 mm LiCl, 1 mm EDTA, 1% Nonidet P-40, 1% deoxycholate) and twice in TE. The detergent conditions in wash buffer II for the specific antibodies used were the following: CBP (sc-369) DetI; GCN5 (sc-6303) DetI; PolII (sc-899) DetII; TFIIB (sc-225) DetI; TFIIH (sc-292) DetI; MED1 (sc-5334) DetII; MED23 (sc-5378) DetII; CDK8 (sc-1521) DetII; MED13 DetII; MED17 (sc-12453) DetII; MED25 (9C2) DetII; CPSF (sc-17289) DetII; CstF-64 (sc-16473) DetII; Ac-H4 (06-866) DetI; Ac-H3K9 (06-942) DetI; trimethyl-H3K4 (07–523) DetI; and dimethyl-H3K79 (07–366) DetI. Bound protein-DNA complexes were eluted in 150 µl of TE/1% SDS, and the formaldehyde cross-link was reversed at 65 °C overnight followed by addition of 1 μl of Proteinase K (Roche Applied Science, 15 mg/ml) and incubation for 1 h at 56 °C. After phenol-chloroform-isoamyl alcohol extraction the DNA was recovered by ethanol precipitation using glycogen (Sigma, 10 µg) as a carrier. After 30 min of centrifugation at 14,000 rpm at 4 °C, the DNA pellet was washed with 70% ethanol, air-dried for 15 min, and resuspended in 40  $\mu$ l of TE. The precipitated DNA was generally analyzed by radioactive PCR. 4  $\mu$ l of template was used in a 50- $\mu$ l reaction that included 0.1  $\mu$ l of radioactive  $[\alpha^{-32}P]dCTP$  (Amersham Biosciences, 3,000 Ci/mmol, final dNTP concentrations in the PCR were 16  $\mu$ M). 1% of input DNA was subjected to PCR amplification as a reference. The PCR reaction optimized for a read-out in the linear range consisted of 27 duty cycles with 30 s for denaturing, annealing, and elongation steps, with the exception of the last cycle when the elongation time was prolonged to 5 min. The amplicons were separated on a 6% native polyacrylamide gel and visualized by autoradiography. The primers used for  $V\beta12-3$  to analyze the promoter were 5'-TGCCAACTATAT-

CCATCTGCACC and 5'-GAGTGGTAAACTCGAGTCTA-ACT. 5'-AGGCGTGTACGGTGGGAGGCC and 5'-AGGCT-GGATCGGTCCCGGTGT were used on the CMV promoter. Proteins on the luciferase open reading frame were detected with 5'-TTCATAGCTTCTGCCAACCGA and 5'-AATGGA-AGACGCCAAAAACAT. 5'-TGATACCCAGTAGTAGA-GTGG and 5'-CAGCAGGAAAAGGACAAGCAG were used on the oriP. For real-time PCR analysis a GeneAmp 5700 sequence detection system instrument (Applied Biosystems) was employed using a standard program for primers with a melting temperature of  $\sim 60$  °C. Levels of immunoprecipitated DNA are given relative to input DNA as determined by a calibration function.

GST Pulldown Assay-VP16 pulldown assays were performed essentially as described previously (18). HeLaS3 extracts were adjusted to 25 mm Hepes-KOH, pH 7.6, 100 mm KCl, 0.1% Nonidet P-40, 1 mm DTT, 0.2 mm EDTA, 10% glycerol, 0.2 mm PMSF and incubated in siliconized Eppendorf tubes with VP16 derivatives fused to GST and immobilized on glutathione-Sepharose at concentrations of 1 mg/ml for 16 h at 4 °C. After four washes with 50 column volumes of HEGN100 buffer (25 mm Hepes-KOH, pH 7.6, 100 mm KCl, 0.1% Nonidet P-40, 1 mm DTT, 0.2 mm EDTA, 10% glycerol, 0.2 mm PMSF) the bound proteins were eluted with SDS buffer and analyzed by immunoblotting.

Immunodepletion of Nuclear Extracts-Nuclear extracts were depleted using anti-MED15 and anti-MED25 rat monoclonal antibodies, MED1 rabbit antiserum (sc-8998, Santa Cruz Biotechnology, Santa Cruz, CA), and CDK8 goat antiserum (Santa Cruz sc-1521) cross-linked with dimethyl pimelimelidate to protein A-Sepharose beads (MED1) or protein G-Sepharose beads (MED15, MED25, and CDK8), essentially as described (27). 100  $\mu$ l of nuclear extracts was adjusted to 20 mм Tris-HCl, pH 6.8, 150 mм KCl, 0.1% Nonidet P-40, 1 mм DTT, 0.2 mm EDTA, 10% glycerol, 0.2 mm PMSF and incubated twice for 3 h with 20 µl of antibody-bound protein A- or G-Sepharose beads at 4 °C. The protein concentration in HeLa nuclear extracts was 8-12 mg/ml and 5 mg/ml in Jurkat nuclear extracts (prepared by standard procedures). The different cell extracts yielded very similar results.

Immunoprecipitation—HeLa nuclear extracts were adjusted to 20 mm Tris-HCl, pH 7.3, 150 mm KCl, 0.1% Nonidet P-40, 1 mм PMSF, 1 mм DTT, 0.2 mм EDTA, 0.2 mм PMSF and incubated with the respective antibody coupled to protein G-Sepharose beads for 16 h at 4 °C (MED15 and MED25 (as described in Refs. 19 and 27, respectively) and CstF64 (Santa Cruz sc-16473)). The rat monoclonal antibody 83M-9A12 was used (provided by E. Kremmer) as an isotype control for the rat monoclonal antibodies (MED15 and MED25). Normal goat serum (Santa Cruz sc-2043) was used as an isotype control for the goat polyclonal CDK8 antibody. Beads were washed three times with 50 column volumes of IP buffer (20 mm Tris-HCl, pH 7.3, 150 mm KCl, 0.1% Nonidet P-40, 1 mm PMSF, 1 mm DTT, 0.2 mm EDTA, 0.2 mm PMSF), and bound proteins were analyzed on Western blots.

Solid-phase Assay—The DNA template was amplified by PCR from the vector pGLMRG5, which stems from pMRG5, but contains a luciferase gene in place of the G-free cassette. The promoter comprises five GAL4 binding sites immediately upstream of a synthetic human immunodeficiency virus/major late core promoter, as described previously (28). Primers: 5'-GCAT-TCTAGTTGTGGTTTGTCCAA (biotinylated) and 5'-GC-CGGGCCTTTCTTTATGTT. The 412-bp template contains the core promoter downstream of the five GAL4 sites flanked by an upstream linker region (5') and 91 bp of the luciferase coding region (3'). The template was purified on 1% agarose gels and recovered using a gel band purification kit (Amersham Biosciences).

Biotinylated DNA templates were coupled to paramagnetic Streptavidin beads (Promega) as follows: the beads were washed twice in B&W buffer (5 mm Tris-HCl, pH 7.5, 1 mm EDTA, 1 M NaCl, 0.003% Nonidet P-40), then resuspended in B&W buffer, and 8.5 ng of biotinylated DNA (in TE with 1 M NaCl) template was added for each microgram of magnetic beads. After shaking for 30 min at room temperature, beads were washed once in B&W buffer containing 0.5 mg/ml BSA (Sigma, fraction V). Beads were resuspended at a concentration of 1 mg/ml in buffer A (150 mm potassium glutamate, 20 mm Hepes-KOH, pH 8.2, 5 mm MgCl<sub>2</sub>, 10 mm DTT, 0.025% Nonidet P-40, 0.5 mg/ml BSA (Sigma, fraction V), 0.2 mm PMSF) plus extra 5 mg/ml BSA (Sigma, fraction V) and 5 mg/ml polyvinylpyrrolidone (Sigma) and incubated for 15 min at room temperature. The beads were then washed three times with buffer A.

A typical pre-initiation complex assembly reaction was conducted in a total volume of 100  $\mu$ l containing: beads bound to 600 ng of DNA (2.4 pmol), 200 ng of Gal4-VP16 (2 μl in BC400 containing 100  $\mu$ M Zn<sup>2+</sup>), comprising the C-terminal 147 amino acids of the Gal4 DNA-binding domain, linked to the complete VP16 activation domain (amino acids 411–490), 2 μg of poly(dGdC), and 500 μg of HeLa or 200 μg of Jurkat nuclear extract, in transcription buffer (27) in which the potassium ions were adjusted with 1 M potassium glutamate to 150 mm.

After a 30-min incubation at 30 °C the complexes bound to the DNA template were concentrated with a magnet and washed twice with 200  $\mu$ l of buffer A. Nucleotides were added in a volume of 100 µl of buffer A at a final concentration of 500  $\mu$ M to 1 mM. After incubation at 30 °C for 20 min bead samples were concentrated with a magnet and washed twice with 200  $\mu$ l of buffer A. Bound proteins were eluted, separated on 12% SDS-PAGE gels, and analyzed by Western blotting.

#### **RESULTS**

An Inducible Tet-VP16-based in Vivo System as a Model for Transcription Complex Assembly at Class II Genes—The Tet-VP16 system was employed as a model to dissect the molecular processes during gene activation (29). The version employed here includes a mutated Tet Repressor (tetR') moiety that recognizes Tet operator sites (tetO) upon interaction with the antibiotic effector doxycycline (Tet-on). EBV-derived vectors carrying the viral origin of replication (oriP) and an expression cassette for the viral EBNA1 protein served as reporters (schematically shown in Fig. 1A). These features facilitate stable replication of low copy numbers of the plasmid in phase with the mammalian cell cycle in human cells (30). Two alternative promoters were employed in this investigation. The plasmid



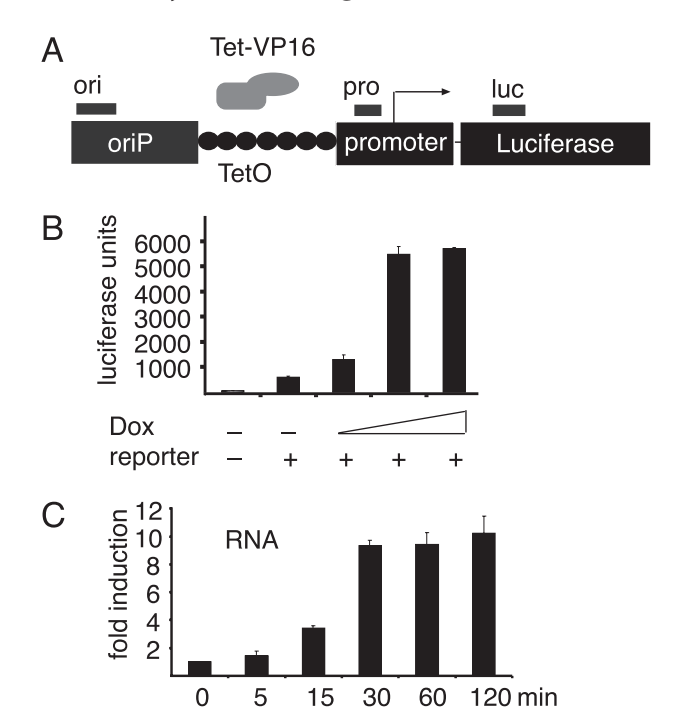


FIGURE 1. A conditional Tet-VP16 EBV vector-based model system for gene activation. A, schematic representation of the inducible EBV vectors and relative position of PCR amplicons. The amplicons for ChIP are located between positions -247 to -430 relative to the transcription start site (promoter), in the luciferase open reading frame (positions +532 to +735) and at the origin of replication, directly adjacent to the family of repeats element. B, representative luciferase analysis of HeLa cells, minus and plus a stable TetOV $\beta$ 12-3 plasmid vector (indicated as reporter) and following the induction of Tet-VP16-binding with 0.1, 1.0, and 10  $\mu$ g/ml doxycycline. C, kinetics of luciferase mRNA synthesis on V $\beta$ 12-3 normalized to chromosomal actin mRNA.

pTU10 contains seven multimerized Tet-operator sites 500 bp upstream of a rearranged T-cell receptor V $\beta$  promoter subtype 12-3 (Fig. 1A). In previous investigations the V $\beta$ 12-3 promoter was shown to display moderate activity in T- and HeLa cells (31). A HeLa cell line stably replicating pTU10 and constitutively expressing a Tet repressor fused to the intact C-terminal activation domain of VP16 was generated. Doxycycline treatment induced luciferase expression (Fig. 1B) without detectable toxic effects on cell growth in the range of  $0.01-10 \mu g$  (per milliliter of medium). Nearly saturating luciferase levels were consistently observed at concentrations of 1 µg/ml, with a further slight increase at 10  $\mu$ g/ml (Fig. 1*B*). Quantitative reverse transcription-PCR of luciferase mRNA showed detectable levels after 15 min of induction that reached steady-state levels after  $\sim$ 30 min (Fig. 1*C*).

The second EBV-based vector carries two bidirectional CMV core promoter regions, with a central Tet-operator element in between, driving expression of luciferase and enhanced green fluorescence protein in opposite directions. This plasmid also expresses a Tet-VP16 molecule comprising multimerized minimal activation elements of VP16 (32). Induction levels were in the range of 100- to 400-fold at the CMV promoter (an example is shown in supplemental Fig. S1).

VP16-dependent Assembly of Pre-initiation and Post-initiation Complexes—Having functionally established a rapid response to VP16, we next investigated the consequences at the level of transcription complex formation using a ChIP assay. The primer pairs used for ChIP-amplified fragments were located between the Tet sites and the V $\beta$ 12-3 core promoter (positions -430 to -247) or directly at the CMV core promoter region. These amplicons, subsequently referred to as promoter amplicons, thus monitor binding of transcription factors to both the regulatory and the core promoter region. Regulatory sites and the promoter are too close to each other on the EBV plasmids to be unambiguously distinguished within the resolution of the preparations (note that the plasmids tend to be more resistant to sonification than chromosomal DNA). In addition, control amplicons were established in the luciferase gene (luc, positions +532 to +735) and in the origin of replication (ori, located adjacent to the family of repeat element) present in both plasmids (see Fig. 1A). Conditions were established for these three primer pairs that generated PCR amplicons in the linear range at a defined input DNA concentration. All subsequent ChIP experiments were conducted under standardized conditions as described in detail under "Experimental Procedures." ChIP experiments were repeated at least three times with independent biological samples.

The Vβ12-3 and CMV cell lines were induced with doxycvcline for 30 min, and the assembly of the RNA polymerase II machinery was monitored by ChIP. We initially used antibodies directed against TFIIB, TFIIH, RNA polymerase II (RNAPII), and the Mediator subunit MED25. RNAPII is expected to associate with the promoter and coding regions. TFIIB serves as a marker for active early pre-initiation complexes, whereas TFIIH monitors the late phase of PIC formation, when the promoter is opened and RNAPII moves from the start site into coding regions.

We observed significant binding of GTFs, RNAPII and MED25, to promoters in the induced situation (Fig. 2A). Before induction, GTFs and RNAPII were undetectable. One exception to this is the low levels of TFIIH seen at the basal V $\beta$ 12-3 promoter. Furthermore, RNAPII was detected in the luciferasecoding region at V $\beta$ 12-3 and to a lesser extent in the CMV plasmid. This presumably relates to the higher basal activity of  $V\beta$ 12-3 compared with CMV. RNAPII, but none of the general factors or Mediator, was detected in the coding region after induction with doxycycline (*middle panel* of Fig. 2*A*).

Unfortunately, the available antibodies failed to immunoprecipitate Tet-VP16 at the Tet DNA element. This is presumably due to the tight packing of the small activation domain into target protein complexes. Based upon (i) the ChIP analysis and (ii) the doxycycline dependence of transcription activation (Fig. 1, B and C), we nevertheless conclude that Tet-VP16 binds to the gene. The activation domain of VP16 is known to act promiscuously and over large distances. This may explain why minor amounts of RNAPII were detected at the (~2 kb distant) oriP control region (right panel, Fig. 2A). A reason for this may be the presence of cryptic promoters. In an attempt to obtain quantitative information about the different levels of RNAPII at promoter versus origin regions, real-time PCR analyses were performed. It revealed low but detectable amounts of RNAPII at both the origin and the promoter region in the non-induced situation (Fig. 2B). These low levels of RNAPII were not detectable in the more qualitative and less sensitive gel-based PCR analysis (Fig. 2A). Activation by doxycycline led to an  $\sim$ 2-fold



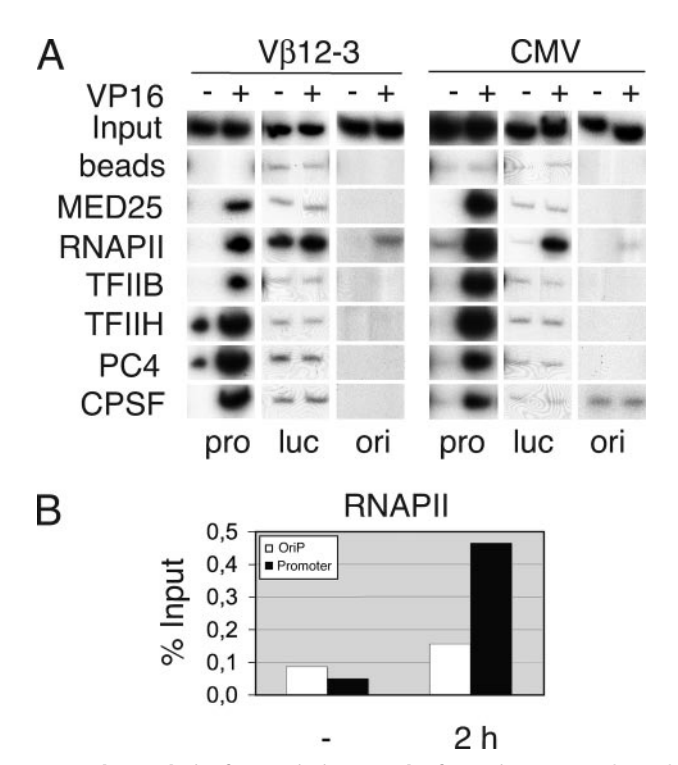
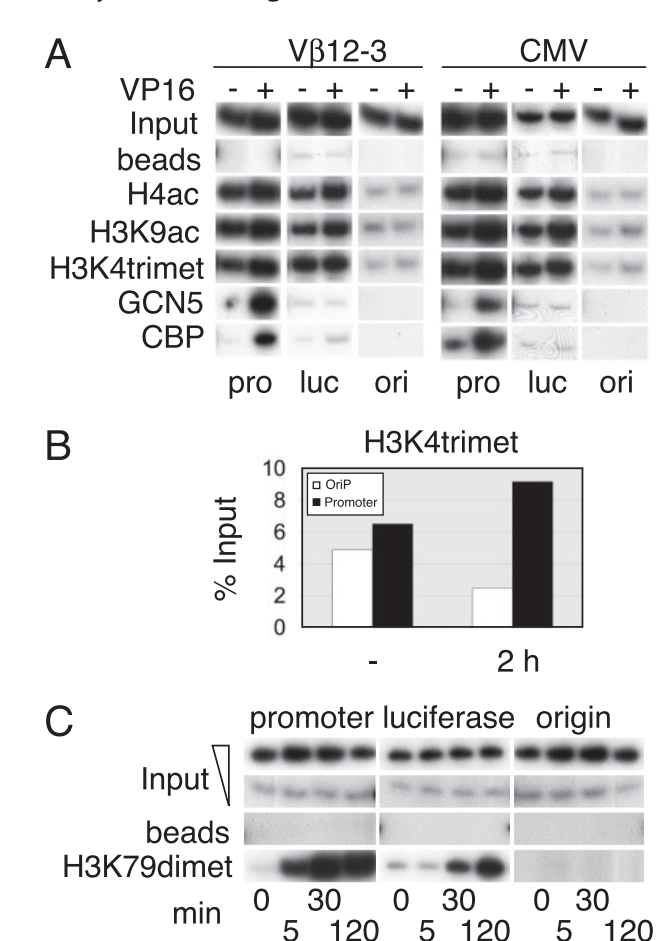


FIGURE 2. ChIP analysis of transcription complex formation. A, VP16-dependent recruitment of RNA polymerase II transcription factors to the  $V\beta12-3$  (left panel) and the CMV (right panel) promoters 30 min after induction of Tet-VP16 with doxycycline (1  $\mu$ g/ml medium). Promoter (pro) regions were compared with gene coding (luc) and origin of replication (ori) regions (see Fig. 1 for their relative positions). Representative inputs of 1% are shown here and in the following figures unless indicated otherwise. B, real-time PCR analysis of RNAPII occupancy on the origin versus the CMV promoter region, before and after a 2-h induction with doxycycline. The VP16-dependent minor changes of RNAPII at the origin are within the experimental error of the two methods and the two independent biological samples (A, right panel, and B).

increase of binding at oriP as compared with a 9-fold enhancement at the promoter region (Fig. 2B). The quantitative experiment clearly shows that VP16 predominantly activates the promoter of the reporter gene. This qualifies the ori amplicon in general as a suitable control and indirectly supports the conclusion that Tet-VP16 binds to the Tet operator as expected.

Another previously identified target of VP16 is positive cofactor 4 (PC4). PC4 has been proposed to function early and late in initiation, where it activates transcription via recruitment of TFIID and TFIIH (10, 33). PC4 can also repress transcription via direct binding to open promoter regions (34). Like the GTFs and Mediator, PC4 association with the promoter was induced by VP16 within 30 min (Fig. 2A). A previously noted co-occupancy with the elongating RNAPII in yeast was not confirmed in this particular mammalian model (35). PC4 has been further suggested to associate with the RNA end formation machinery in yeast (36). Hence, we tested the cleavage and polyadenylation complex using the CPSF160 subunit as an indicator for its presence. CPSF160 was indeed detected at the promoter. Of note, like PC4 and the other factors, CPSF was absent from the coding region of the luciferase gene where RNAPII is readily detectable (Fig. 2A).

Influence of VP16 on the Chromatin Structure—The subsequent ChIP analyses revealed that VP16 recruits both CBP and GCN5 (Fig. 3A). Nevertheless, changes in acetylation at the histone H3 and H4 tails were moderate. This may be due to the



 ${\sf FIGURE\,3.\,ChIP\,analysis\,of\,chromatin\,and\,chromatin\,modifiers\,on\,the\,EBV}$ vectors. A, ChIP was carried out as indicated 30 min after adding doxycycline at the VB12-3 and CMV vectors. B, real-time PCR analysis of H3K4 trimethylation on the origin versus the CMV promoter as indicated. The observed changes of H3K4 trimethylation are within the experimental error of independent biological samples. C, kinetics of H3K79 dimethylation at V $\beta$ 12-3 in comparison to 0.1 and 1% input as indicated. Note the delayed appearance of the histone modification in coding regions.

high basal levels, which are generally seen on the stably replicating plasmids. 4 Similarly, H3K4-dimethyl (data not shown) and H3K4-trimethyl levels were high before induction and were not, or only slightly induced by VP16 (Fig. 3B). Modified histones but not histone acetyltransferases were detected at the origin of replication (Fig. 3A). Quantitative real-time PCR analysis at the CMV reporter confirmed the moderate effects of Tet-VP16 on H3K4 trimethylation (Fig. 3B). It also demonstrated that the radioactive PCR analysis (Fig. 3A) overemphasizes the differences in histone occupancy on the origin versus the promoter region (Fig. 3A).

Another histone modification that correlates with active transcription is the methylation of lysine 79 of H3 (H3K79). In contrast to the histone tail modifications described above, dimethylation at H3K79 was markedly enhanced after induction by VP16, reaching a maximum after 30 min. The H3K79-dimethyl signal was undetectable in the basal state and appeared to be propagated with time from the promoter into the lucifer-



<sup>&</sup>lt;sup>4</sup> T. Uhlmann, S. Boeing, M. Lehmbacher, and M. Meisterernst, unpublished observation.

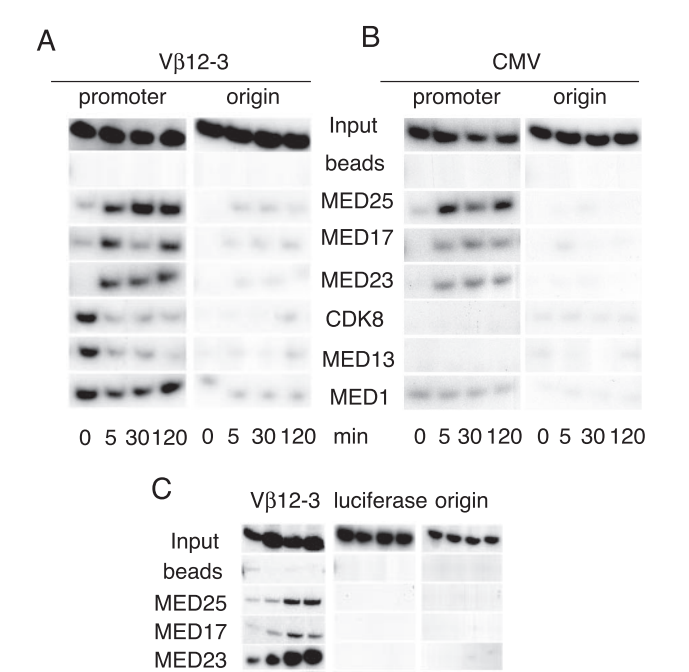


FIGURE 4. Kinetic ChIP analysis. A, time course of factor binding at  $V\beta$ 12-3 at the indicated time points after addition of doxycycline. B, time course of factor binding at CMV templates at the indicated times after adding doxycycline. Note that while core Mediator subunit occupancy increases, CDK8 and MED13 leave the promoters, and MED1 levels appear constant. C, short-term kinetics of Mediator and RNA polymerase II promoter association on V $\beta$ 12-3.

0135 0135

0135

CDK8

MED<sub>1</sub>

**RNAPII** 

ase open reading frame. In parallel, the oriP region remained in a non-modified state (Fig. 3C).

VP16 Mediates the Association of a Specific Mediator Complex—There is substantial evidence from previous investigations that VP16 binds to, and efficiently recruits Mediator complexes (12, 18, 19, 25, 37). We next asked whether MED25 enters the gene with other Mediator subunits and, more generally, whether the Mediator subunits enter the promoter synchronously in living cells. Among the available antibodies those against MED1 (TRAP220), MED13 (TRAP240), MED17 (TRAP80), MED23 (TRAP150), MED25 (ACID1), and CDK8 proved to function reasonably well in ChIP assays. These were therefore used for a time-dependent analysis of complex formation. Within 5 min after adding doxycycline, levels of Mediator subunits MED17, MED23, and MED25 increased significantly at the promoter region. The minor amounts of Mediator detected at the origin of replication were not consistently seen (compare Fig. 4 (A and B) and supplemental Fig. S2). Steadystate levels were reached shortly thereafter. Other subunits such as MED6 and MED21 (SRB7) followed the pattern of MED17, MED23, and MED25 (data not shown). In contrast, MED1 was seen at V $\beta$ 12-3 before induction, yet levels remained unchanged following the addition of the inducing compound (Fig. 4A). Both CDK8 and MED13 were also found in the non-induced situation, but these factors apparently dissociate from the V $\beta$ 12-3 promoter upon induction (Fig. 4A, bottom panels).

Similar results were obtained at the CMV promoter, but here CDK8 and MED13 subunits are undetectable before gene induction (Fig. 4B). The reason for the presence of CDK8 and MED1 at the non-induced V $\beta$ 12-3 is unclear at present but may relate to the fact that this promoter is under the control of ubiquitous proximal activators (i.e. cAMP-response elementbinding protein (31)). Although this aspect needs to be examined further, the data collectively argue for the establishment of a specific steady-state Mediator containing the head module but lacking parts of the CDK8 module, under the control of VP16 at both promoters.

Subsequently, a short term kinetic analysis was conducted with the intention of further dissecting the assembly process (Fig. 4C). This experiment did not reveal significant differences in the time course of promoter association between different Mediator subunits. All subunits rapidly associated with  $V\beta12-3$ . Mediator was detected 1 min after induction and reached saturating levels within 5 min (Fig. 4C). The appearance of the associating Mediator subunits and disappearance of CDK8 appeared to be temporally correlated.

Association of Cleavage Stimulatory Factor with VP16—To further investigate the binding of cleavage polyadenylation factor, a kinetic analysis was conducted using the currently available antibodies against CstF64 and CPSF160. Both factors appear to enter the gene region in a temporally correlated manner, but with a delay compared with Mediator and RNAPII (Fig. 5A). In an attempt to unravel the underlying molecular mechanism we next asked whether gene interactions require contacts to the Mediator and/or the activator VP16. Immunoprecipitations were conducted using MED15 and MED25 antibodies and suitable isotype controls (Fig. 5B). Although the CstF64 antibody worked in immunoprecipitations and Western blots, CPSF160 remained inefficient in Western blots. Hence, CstF64 was used as a measure for the complex. CstF64 was not detected in the bound Mediator fractions under conditions of low and intermediate stringency where Mediator components co-precipitated with each other (Fig. 5*B*, *lanes 5* and 6). Given that the IP was conducted at near physiological salt conditions these results minimally argue against a strong interaction of CPSF/CstF and Mediator. Next, GST pulldown experiments were conducted with VP16. Full-length VP16 activation domain (VP16) and the subdomains H1 and H2 fused to GST, as well as functional mutations in H1 and H2, which render the activator inactive in mammalian cells (described in Ref. 18) were compared (Fig. 5C). CstF64 co-precipitated with the intact VP16 activation domain and with H2, but not with a triple FFF mutation in H2 and not with the H1 region alone. We conclude that the VP16 activation domain but not Mediator binds directly or indirectly to components of the RNA 3'-end formation complex.

VP16-dependent Recruitment of a Specific Mediator Variant in Vitro-According to the previous biochemical analyses VP16 binds Mediator independently of its association with CDK8 (19, 25) raising questions about the absence of CDK8 *in* vivo. This could be caused by either a sub-stoichiometric distribution of CDK8 in Mediators or a mechanism that leads to its removal, *i.e.* during transcription. To examine these hypotheses we used biochemical immunodepletion assays. Contrary to



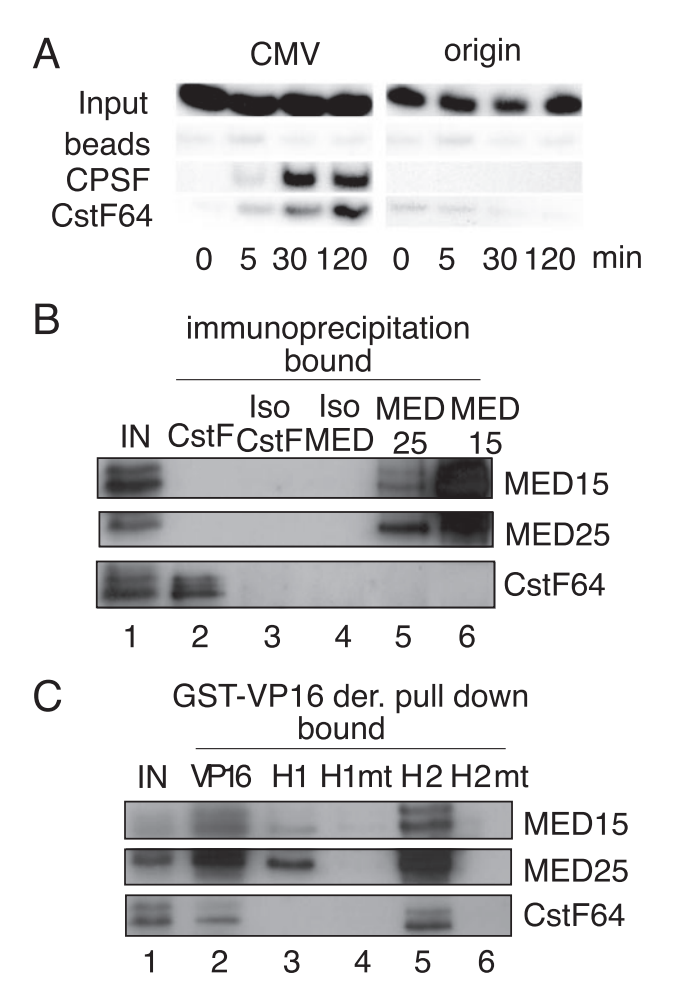


FIGURE 5. Kinetics of CPSF/CstF association and binding to VP16. A, kinetics of recruitment of CPSF160 and CstF64 to the CMV promoter and ori control. B, Western blot of Mediator and CstF64 IP compared with input extract (IN) and isotype (Iso) controls at 150 mm KCl. Mediator-CstF interactions were also not detected under less stringent (100 mm KCI) conditions (data not shown). C, binding of the indicated Mediator components and cleavage stimulatory factor CstF64 to immobilized GST-VP16. VP16 represents the fulllength activation domain (amino acids 411-490), H1 (amino acids 411-452), H2 (amino acids 453-490), H1mt is F442P, and H2mt F473A,F475A,F479A. Equal amounts of immobilized GST VP16 derivatives (der) were used (data not shown).

previous biochemical analyses that employed purified Mediator preparations, these were conducted in nuclear extracts (38, 39). Monoclonal antibodies directed against MED15 and MED25 and polyclonal antibodies against CDK8 and MED1 were used to deplete standard Dignam HeLa or Jurkat nuclear extracts of the complexes associated with them. Double depletions ( $\Delta\Delta$ ) were applied to optimize the efficiency. TBP served as a loading control (Fig. 6A). MED15 depletion reproducibly removed all MED25 as well as other Mediator core subunits but left behind a minor fraction of CDK8. This confirms the earlier notion of Conaway and colleagues (13) that MED25 is fully associated with Mediator in nuclear extracts. It further shows that initially most of the CDK8 exists in a Mediator-bound form. CDK8 depletion, while being highly efficient for the antigen, removed a smaller fraction of MED25 and other Mediator subunits. MED25 depletion left behind a larger fraction of CDK8. MED1 depletion removed all MED7 but left behind a fraction of MED15, MED25, and CDK8. These findings indicate

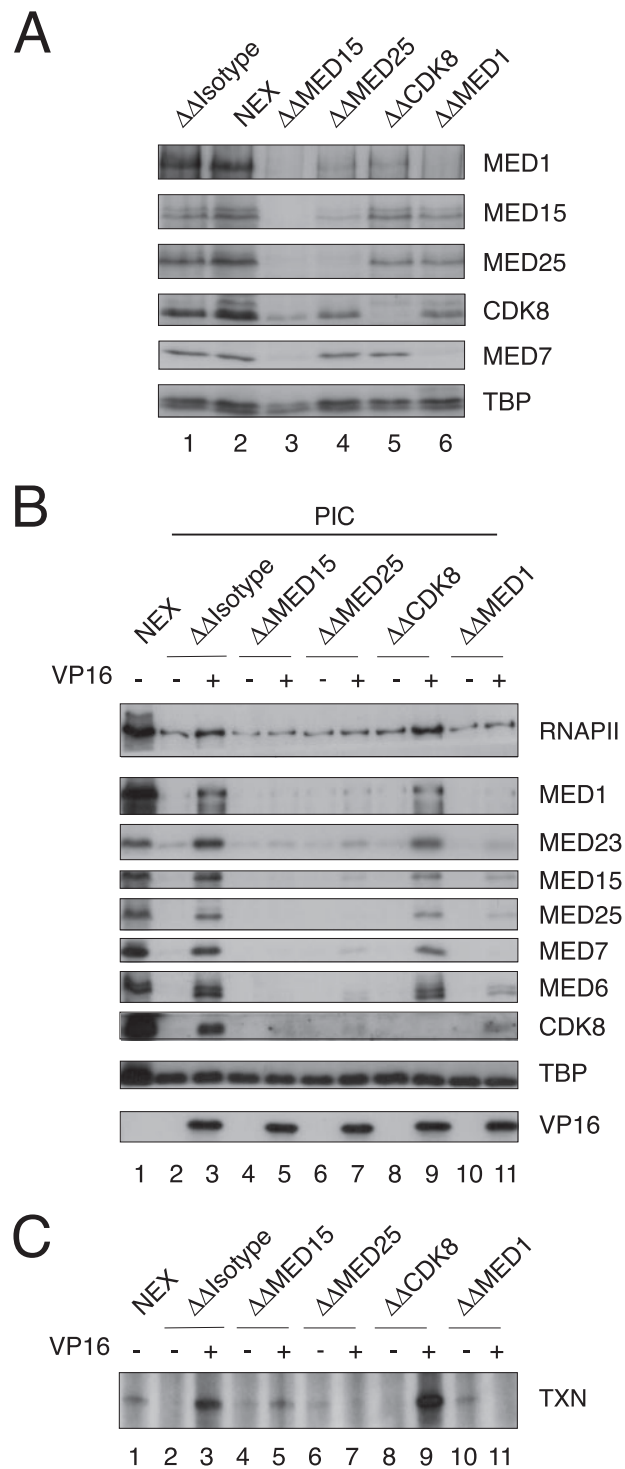


FIGURE 6. Biochemical and functional analyses of extracts depleted for variant Mediator complexes. A, Western blot analysis of double immunodepleted HeLa extracts using the antibodies against the indicated Mediator subunits. HeLa extracts were used because these produce better signals because of high protein amounts. Jurkat nuclear extracts led to an essentially identical picture (data not shown). B, Western blot analysis of factors bound to immobilized templates upon double depletion with antibodies against the indicated Mediator subunits in the absence and presence of Gal4-VP16 using Jurkat extracts. Lane 1 (NEX) shows a nuclear extract control. PIC (preinitiation complex) indicates analysis of complexes bound to and washed on the immobilized templates (lane 2 to lane 11). C, in vitro transcription analyses of isotype and the indicated Mediator-subunit double depleted Jurkat nuclear extracts on a adenovirus major late promoter carrying five upstream Gal4 binding sites in the presence and absence of Gal4-VP16 as indicated.

that the extracts contain a second MED15-MED25 complex that lacks MED7. This could be a free head module or a larger subcomplex. Notably, the data further suggest that CDK8 is under-represented in the MED25- and MED1-associated Mediators.

To further characterize the subform of Mediator that is recruited by VP16 we subsequently employed solid-phase techniques. HeLa nuclear extracts were incubated with an immobilized DNA fragment comprising five consecutive Gal4 binding sites upstream of a synthetic core promoter and part of the luciferase reporter gene. Transcription complexes were formed in the absence and presence of Gal4-VP16 using extracts depleted of Mediator variants. Bound complexes were washed, and the proteins were eluted, separated by SDS-PAGE, and analyzed in Western blots (Fig. 6B). As a control we used an extract depleted with an isotype antibody. Antibodies directed against the Gal4 DNA binding module served as a loading control. The data show a requirement for MED1-, MED15-, and MED25associated complexes for VP16-dependent binding of Mediator (Fig. 6B). CDK8 depletion reduces the amount of templatebound Mediator but does not prevent its recruitment (lane 9 versus lane 3).

We observed binding of both a basal (lanes 2, 4, 6, 8, and 10) and, in addition, a VP16-dependent form of RNAPII (lanes 3 and 9). The VP16-induced recruitment of RNAPII was closely linked to the binding of active Mediators. Despite the reduction in Mediator levels in  $\Delta\Delta$ CDK8 extracts, RNAPII recruitment remained unaffected (Fig. 6B, lane 3 versus lane 9). On the other hand, TFIIH (Fig. 7A) and TBP binding (Fig. 6B) is entirely independent of activator and Mediator.

The data suggest that VP16 recruits an active Mediator containing MED1, MED15, and MED25, perhaps together with RNAPII (40). Its activity was subsequently confirmed by *in vitro* transcription analyses (Fig. 6C). Depletion of MED1, MED15, or MED25 abolished transcription activation by VP16. Contrary to this, but in agreement with the previous biochemical analyses (39), CDK8 depletion did not reduce transcription efficiency, but rather slightly increased the number of run-off transcripts (lane 3 versus lane 9). Comparison of the transcription output with the binding analysis (Fig. 6, B versus C) supports the previous notion that CDK8 complexes are refractory to transcription activation (38, 41).

The *in vitro* experiment argues for an active role of MED1 in transcription. This was not deducible from the ChIP analysis, although it did not exclude a contribution (Figs. 3 and 4). Another difference between the *in vivo* and *in vitro* analyses is the observation that limited amounts of CDK8 bind to the promoter in vitro, whereas CDK8 remains undetectable in vivo.

We thus asked whether the kinase is further dissociated under conditions facilitating transcription. Toward this end we monitored binding of transcription factors to an immobilized template in the presence and absence of nucleotides. This initially revealed template-dependent recruitment of low amounts of a Mediator in the absence of activator (Fig. 7, lane 2 versus lane 3). This Mediator variant lacks significant amounts of MED25 but contains MED1, MED7, MED15, and CDK8. The binding of this variant, which may represent a basal (27, 42) or an inactive form (12, 43), or a mixture of both, was less evident

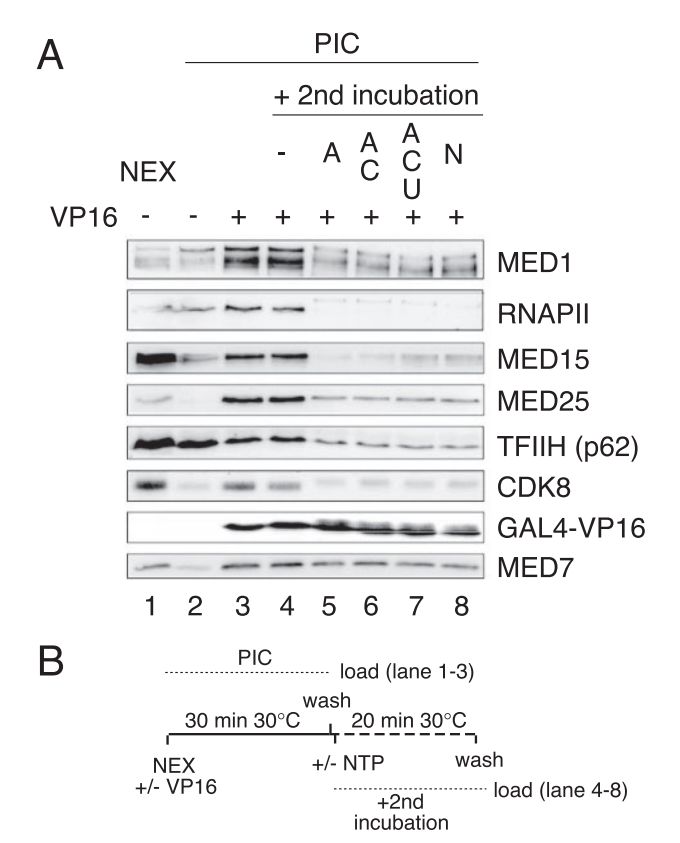


FIGURE 7. Characterization of transcription complexes formed under the control of GAL4-VP16 on immobilized templates and influence of nucleotides on their composition. A, Western blot analysis of HeLa extract (NEX) (25% of material relative to the bound fraction, lane 1) and factors bound to immobilized templates (PIC formation) in the absence and presence of saturating amounts of GAL4-VP16 using the indicated antibodies (right). Several reactions (lanes 4-8) were subjected to a second incubation period with buffer only (lane 4), ATP (A, open complex formation, lane 5), ATP and CTP (AC, allowing transcription to position 2), ATP, CTP, and UTP (ACU, allowing transcription to position 29) and all four NTPs (N, 91-bp run-off transcript conditions). B, schematic protocol for this solid-phase assay. PIC, preinitiation complex formation; NEX, nuclear extract.

in the previous analysis (Fig. 6B), probably because lower protein amounts were used in the first analysis.

In agreement with the data above, Mediator binding was further strongly induced by VP16. In parallel binding of TFIIH was essentially unaffected (lane 2 versus lane 3). Remarkably, among the different Mediator subunits, the enrichment of MED25 by VP16 is most pronounced (compare lane 2 and lane 3). CDK8 was again co-recruited with Mediator to the template, as was MED1. However, in agreement with analysis of the Mediator complexes in solution (Fig. 6A), relative levels of recruited MED25 (and MED7) exceeded those of CDK8 and of MED1 (compare lane 2 and lane 3).

In extension to the above solid-phase experiment (Fig. 6B), the preformed complexes at the immobilized template were subsequently subjected to a second incubation procedure (see scheme in Fig. 7B), which included ATP and different combinations of nucleotides (Fig. 7A, lanes 4-8). Under these conditions we consistently observed a loss of the tail subunits MED15, and of subunits MED1 and CDK8, relative to the middle and head module components MED7 and MED6 (data not shown). Also GTF levels dropped compared with the amount of bound GAL4-VP16, which remained constant. Of note, the

most significant loss of MED15 and CDK8 was seen in the presence of ATP alone (lane 4 versus lane 5). For reasons unknown, this phenomenon required physiological (0.5–1 mm) ATP concentrations and was not seen at the concentrations (100  $\mu$ M or below) routinely employed for transcription assays in our laboratory (27). Adding all four NTPs (lane 8) yielded similar results, although the effects on MED15 disassembly appeared to be attenuated (compare lane 5 with lane 8). Conditions that facilitate the formation of dinucleotides at the major late promoter (ATP and CTP, lane 6), or the formation of short 29-bp transcripts (the template carries only A, U and T bases between positions 1 and 29 downstream of the transcription start site, lane 7) yielded intermediate results. In parallel, the largest subunit of RNAPII (and perhaps also CDK8) apparently becomes modified (lane 4 versus lane 5).

Curiously, in the presence of physiological concentrations of ATP, CDK8 but not MED7 or MED25 amounts dropped to levels seen in the absence of activator (lane 5 versus lane 2). It is thus tempting to speculate that there is a net loss of CDK8 depending on a yet to be defined energy-dependent process. However, interpretation of the solid-phase experiment is complicated by the fact that it monitors several superimposed and perhaps independently controlled complexes. These are according to the previous data minimally, (i) a form of Mediator recruited in the absence of activator, (ii) the activated MED25core Mediator, and (iii) a MED25-associated tail complex (Fig. 6, A and B). Moreover, both Western blot and ChIP monitor relative protein amounts. They do not define stoichiometries of complexes.

Collectively, both the ChIP and the in vitro data presently underline the previous notion (19) that VP16 indeed utilizes a MED25-associated Mediator. A novel aspect is the relative deficiency of this Mediator in CDK8. Further novel, our data suggest that Mediator composition changes on genes in an energydependent manner, leading to a loss of tail subunits and of CDK8 relative to MED7. For the first time we provide evidence for the existence of free MED25-associated Mediator tail fragments.

#### DISCUSSION

A Model for Gene Activation in Mammals—In this investigation the Tet repressor DNA-binding module fused to the activation domain of VP16 was used as a simple model for gene activation by a single strong activator in living cells. Chromatin immunoprecipitation analyses of two different promoters provided a detailed picture with respect to both transcription complex formation and the manipulation of chromatin structure. Consistent with previous biochemical investigations, Mediator (12, 19, 25), CBP (18), GCN5/TFTC (17), and PC4 (44) localized to the promoter following induction by VP16. Comparison of ChIP data with biochemical experiments provided insights into both functional intermediates and the final composition of the active MED25-associated Mediator, which apparently lacks CDK8. Consistent with earlier reports (compare references in the introduction) the entire transcription machinery rapidly appeared at the promoter upon activation of Tet-VP16. Novel observations include the binding of CPSF/CstF components to regulatory regions and the notion of significant de novo H3K79

methylation at the promoter region following transcription activation.

Evidence for a Transcription-RNA Processing Complex at Gene Regulatory Regions-An association of CPSF/CstF complexes with the general factor TFIID at promoters has been proposed previously (45). Our data argue for the relevance of this observation by adding *in vivo* evidence for the assembly of two components of CPSF/CstF with two different promoters. Beyond the previous study our data suggest that the activator, VP16, recruits RNA 3'-end formation factors to regulatory sites. CPSF/CstF complexes were not detected in the coding region, arguing against a model of propagation through the coding region (45). This scenario was generally confirmed in the context of cellular genes and so may be generally relevant.<sup>5</sup>

In preliminary investigations, binding of CstF64 to the in vitro immobilized templates was found to be inefficient (data not shown). However, the templates used in vitro presently lack the RNA 3'-end formation elements. Moreover, mRNA synthesis is temporally correlated with the delayed appearance of CPSF/CstF at the regulatory region (see Figs. 1C and 5A). It will be of tremendous interest to investigate whether both the activator and transcription through these elements are needed for efficient association of CPSF/CstF in vivo. Presently our data indeed support a model where RNA 3'-end formation, mediated by activator contacts, takes place near the regulatory region.

Chromatin Modulation by VP16—The observation that the histone acetyltransferases CBP and GCN5 are rapidly recruited by VP16 to promoters is generally in line with both the biochemical analyses (18) as well as the in vivo characterization of lac-VP16 proteins on an integrated multimerized response element (46 – 48). Nevertheless, the corresponding changes at the histone tails remained low on the episomal plasmids. This is presumably due to high basal acetylation and methylation activity on the corresponding nucleosomes (30, 49). Both the origin of replication and the active genes may contribute to this active status of the chromatin before binding of Tet-VP16. In conclusion, the recruitment of CBP and GCN5 by VP16 might have a much more pronounced functional impact in a less active chromatin environment.

In contrast to the acetylation and H3K4 trimethylation, the dimethylation of lysine 79 in H3 was (i) undetectable prior to activation with VP16 and (ii) strongly induced by the activator. The preliminary data indicate that this histone modification may be slowly propagated into coding regions after induction. This occurs in a background of other active genes on the plasmids and may relate to the strength of VP16, which induces the CMV promoter several hundred-fold (supplemental Fig. S1). In Drosophila melanogaster the occurrence of dimethylated lysine 79 of histone H3 generally correlates with active genes (50). In mammals, methylation of H3K79 by the responsible methyltransferase Dot1L was so far shown to correlate with the function of a few activators, among them leukemia-inducing MLL and CALM-AF10 fusion proteins (Ref. 51 and references therein). Perhaps correlating to this, the VP16 activation



<sup>&</sup>lt;sup>5</sup> T. Albert and M. Meisterernst, unpublished observation.

domain transforms hematopoietic stem cells in a manner indistinguishable from the pathological fusion partners of MLL, if connected to an MLL DNA-binding domain (52).

Establishment of a Core Mediator Lacking CDK8 at Active Promoters in Vivo—In yeast Mediator a CDK8 (SRB10) kinase module containing MED13, MED12, CDK8, and CycC has been implicated in transcription repression (53). However, genomewide ChIP studies suggested that CDK8 is found in the coding region of active and inactive genes (54, 55). Moreover, positive functions of CDK8 have been proposed in the yeast Saccharomyces cerevisiae, which relate to the phosphorylation of the MED2 subunit (56).

Mammalian Mediator complexes enriched for the CDK8 module repress transcription *in vitro* (43, 57). Activation of chromosomal genes is accompanied by exchanging inactive large Mediator complexes, containing the CDK8 module (ARC), with a small and active Mediator complex (39, 58). Further in line with a negative role of CDK8, depletion of CDK8 from isolated Mediator did not diminish transcription activation (38, 39). Moreover, recombinant CDK8 inhibited transcription in reconstituted systems (59). Conversely, there is no definitive evidence for positive functions of CDK8 in mammals. In some studies the behavior of the factor was apparently neutral. For example, CDK8 was found in inactive and active Mediator complexes *in vitro* (Ref. 14 and references therein). At the *Egr1* gene, activation by mitogen-activated protein kinases did not relate to changes in CDK8 levels (60).

Our data confirm and extend the hypotheses invoking a negative role of CDK8, here in VP16-dependent transcription. In extension to previous *in vitro* approaches we used nuclear extracts instead of reconstituted systems, establishing a more physiological context. Our results further suggest that activator-dependent recruitment of RNAPII, in nuclear extracts, is fully independent of the large CDK8 containing Mediators. These data are generally in line with a recent electron microscopy analysis showing mutually exclusive binding of CDK8 and RNAPII to Mediator (61).

On the *RARβ2* gene, dissociation of CDK8 was linked to poly(ADP-ribose) polymerase 1 (62). Although we could detect poly(ADP-ribose) polymerase on the immobilized templates (data not shown) we have presently no evidence based on ChIP for poly(ADP-ribose) polymerase assembly *in vivo*. Instead, the apparent absence of CDK8 *in vivo* is presently best explained (i) by its under-representation in nucleoplasmic Mediator complexes and (ii) by a subsequent ATP-dependent depletion of Mediator components, including CDK8, relative to MED25 and core subunits. As a result the CDK8-containing Mediator complexes are apparently limiting in chromatin. It will be of interest to clarify whether transcription *per se* or another ATP-requiring process is responsible for the observed deficiency of CDK8 in chromatin-bound Mediator complexes (data not shown and Ref. 63).

The *in vitro* analysis lends further support to the hypothesis that multiple Mediator variants exist in mammals (12, 19, 27, 40, 42, 64, 65). Our data provide strong evidence that VP16 utilizes a MED25-associated core Mediator for activation that lacks CDK8. This Mediator joins templates together with an active RNAPII *in vitro*, which perhaps relates it to the Media-

tor-RNA polymerase II holoenzyme, described by Roeder and colleagues (40). Our data further suggest that MED25 is present in a second complex containing MED15 and perhaps CDK8 (Fig. 6A, lane 6 and Fig. 6B, lane 11) but lacking MED1 and MED7. This presumptive Mediator fragment does not facilitate activation by VP16 in vitro. It may thus not relate to the CRSP-Med2 complex, which does lack MED1 but supports activation by VP16 (40, 41). In our analysis, MED1 is recruited, and extracts depleted for MED1 failed to support activation by VP16 (Fig. 6). One explanation could be that the CRSP-Med2 complex is limiting in these nuclear extracts. It will be of interest to investigate whether the constant levels of MED1 seen during activation of the gene *in vivo* result of superposition of binding of a MED1-containing Mediator variant and the subsequent dissociation of tail components (Fig. 7A). Further studies on the structures, functions, and life cycle of Mediators will be critical for an understanding of the control of RNA polymerase II transcription in eukaryotes.

Acknowledgments—We thank G. Bornkam for providing materials, Patrick Cramer and Dirk Eick for advice, and the members of the Meisterernst laboratory for support.

#### REFERENCES

- Wilson, A. C., Freiman, R. N., Goto, H., Nishimoto, T., and Herr, W. (1997) Mol. Cell Biol. 17, 6139 – 6146
- Cousens, D. J., Greaves, R., Goding, C. R., and O'Hare, P. (1989) EMBO J. 8, 2337–2342
- Sadowski, I., Ma, J., Triezenberg, S., and Ptashne, M. (1988) Nature 335, 563–564
- 4. Triezenberg, S. J., Kingsbury, R. C., and McKnight, S. L. (1988) *Genes Dev.* **2,** 718 –729
- Choy, B., Roberts, S. G., Griffin, L. A., and Green, M. R. (1993) Cold Spring Harb. Symp. Quant. Biol. 58, 199–203
- 6. Stringer, K. F., Ingles, C. J., and Greenblatt, J. (1990) Nature 345, 783-786
- Goodrich, J. A., Hoey, T., Thut, C. J., Admon, A., and Tjian, R. (1993) Cell 75, 519-530
- Kobayashi, N., Boyer, T. G., and Berk, A. J. (1995) Mol. Cell Biol. 15, 6465–6473
- Lin, Y. S., Ha, I., Maldonado, E., Reinberg, D., and Green, M. R. (1991) *Nature* 353, 569 – 571
- Fukuda, A., Nakadai, T., Shimada, M., Tsukui, T., Matsumoto, M., Nogi, Y., Meisterernst, M., and Hisatake, K. (2004) Mol. Cell Biol. 24, 6525–6535
- Fondell, J. D., Ge, H., and Roeder, R. G. (1996) Proc. Natl. Acad. Sci. U. S. A. 93, 8329 – 8333
- Naar, A. M., Beaurang, P. A., Zhou, S., Abraham, S., Solomon, W., and Tjian, R. (1999) *Nature* 398, 828 – 832
- Sato, S., Tomomori-Sato, C., Parmely, T. J., Florens, L., Zybailov, B., Swanson, S. K., Banks, C. A., Jin, J., Cai, Y., Washburn, M. P., Conaway, J. W., and Conaway, R. C. (2004) Mol. Cell 14, 685–691
- 14. Malik, S., and Roeder, R. G. (2005) *Trends Biochem. Sci.* **30,** 256–263
- 15. Blazek, E., Mittler, G., and Meisterernst, M. (2005) *Chromosoma* 113, 399-408
- Conaway, R. C., Sato, S., Tomomori-Sato, C., Yao, T., and Conaway, J. W. (2005) *Trends Biochem. Sci.* 30, 250 – 255
- 17. Hardy, S., Brand, M., Mittler, G., Yanagisawa, J., Kato, S., Meisterernst, M., and Tora, L. (2002) *J. Biol. Chem.* **277**, 32875–32882
- 18. Ikeda, K., Stuehler, T., and Meisterernst, M. (2002) Genes Cells 7, 49-58
- Mittler, G., Stuhler, T., Santolin, L., Uhlmann, T., Kremmer, E., Lottspeich, F., Berti, L., and Meisterernst, M. (2003) EMBO J. 22, 6494–6504
- Kraus, W. L., Manning, E. T., and Kadonaga, J. T. (1999) Mol. Cell Biol. 19, 8123–8135



- 21. Kundu, T. K., Palhan, V. B., Wang, Z., An, W., Cole, P. A., and Roeder, R. G. (2000) Mol. Cell 6, 551-561
- 22. Utley, R. T., Ikeda, K., Grant, P. A., Cote, J., Steger, D. J., Eberharter, A., John, S., and Workman, J. L. (1998) Nature 394, 498 - 502
- 23. Ikeda, K., Steger, D. J., Eberharter, A., and Workman, J. L. (1999) Mol. Cell Biol. 19, 855-863
- 24. Neely, K. E., Hassan, A. H., Wallberg, A. E., Steger, D. J., Cairns, B. R., Wright, A. P., and Workman, J. L. (1999) Mol. Cell 4, 649 - 655
- 25. Ito, M., Yuan, C. X., Malik, S., Gu, W., Fondell, J. D., Yamamura, S., Fu, Z. Y., Zhang, X., Qin, J., and Roeder, R. G. (1999) Mol. Cell 3, 361–370
- 26. Gilfillan, S., Stelzer, G., Piaia, E., Hofmann, M. G., and Meisterernst, M. (2005) J. Biol. Chem. 280, 6222-6230
- 27. Mittler, G., Kremmer, E., Timmers, H. T., and Meisterernst, M. (2001) EMBO Rep 2, 808 – 813
- 28. Xie, J., Collart, M., Lemaire, M., Stelzer, G., and Meisterernst, M. (2000) EMBO J. 19, 672-682
- 29. Gossen, M., and Bujard, H. (1995) Bio Techniques 19, 213-216; discussion
- 30. Zhou, J., Chau, C. M., Deng, Z., Shiekhattar, R., Spindler, M. P., Schepers, A., and Lieberman, P. M. (2005) EMBO J. 24, 1406-1417
- 31. Halle, J. P., Haus-Seuffert, P., Woltering, C., Stelzer, G., and Meisterernst, M. (1997) Mol. Cell Biol. 17, 4220 - 4229
- Seipel, K., Georgiev, O., and Schaffner, W. (1994) Biol. Chem. Hoppe-Seyler 375, 463-470
- 33. Kaiser, K., Stelzer, G., and Meisterernst, M. (1995) EMBO J. 14, 3520 - 3527
- 34. Werten, S., Stelzer, G., Goppelt, A., Langen, F. M., Gros, P., Timmers, H. T., Van der Vliet, P. C., and Meisterernst, M. (1998) EMBO J. 17,
- 35. Calvo, O., and Manley, J. L. (2005) EMBO J. 24, 1009-1020
- 36. Calvo, O., and Manley, J. L. (2001) Mol. Cell 7, 1013-1023
- 37. Johnson, K. M., Wang, J., Smallwood, A., and Carey, M. (2004) Methods Enzymol. 380, 207-219
- 38. Wang, G., Cantin, G. T., Stevens, J. L., and Berk, A. J. (2001) Mol. Cell Biol. 21, 4604 - 4613
- 39. Taatjes, D. J., Naar, A. M., Andel, F., 3rd, Nogales, E., and Tjian, R. (2002) Science 295, 1058-1062
- 40. Zhang, X., Krutchinsky, A., Fukuda, A., Chen, W., Yamamura, S., Chait, B. T., and Roeder, R. G. (2005) Mol. Cell 19, 89-100
- 41. Taatjes, D. J., and Tjian, R. (2004) Mol. Cell 14, 675-683
- 42. Baek, H. J., Kang, Y. K., and Roeder, R. G. (2006) J. Biol. Chem. 281, 15172 - 15181
- Sun, X., Zhang, Y., Cho, H., Rickert, P., Lees, E., Lane, W., and Reinberg, D. (1998) Mol. Cell 2, 213-222
- 44. Ge, H., and Roeder, R. G. (1994) Cell 78, 513-523

- 45. Dantonel, J. C., Murthy, K. G., Manley, J. L., and Tora, L. (1997) Nature **389**, 399 – 402
- 46. Janicki, S. M., Tsukamoto, T., Salghetti, S. E., Tansey, W. P., Sachidanandam, R., Prasanth, K. V., Ried, T., Shav-Tal, Y., Bertrand, E., Singer, R. H., and Spector, D. L. (2004) Cell 116, 683-698
- 47. Tsukamoto, T., Hashiguchi, N., Janicki, S. M., Tumbar, T., Belmont, A. S., and Spector, D. L. (2000) Nat. Cell Biol. 2, 871-878
- 48. Tumbar, T., Sudlow, G., and Belmont, A. S. (1999) J. Cell Biol. 145, 1341-1354
- 49. Fivaz, J., Chiarra Bassi, M. C., Pinaud, S., Richman, L., Price, M., and Mirkovitch, J. (2000) Methods Mol. Biol. 133, 167-182
- 50. Schubeler, D., MacAlpine, D. M., Scalzo, D., Wirbelauer, C., Kooperberg, C., van Leeuwen, F., Gottschling, D. E., O'Neill, L. P., Turner, B. M., Delrow, J., Bell, S. P., and Groudine, M. (2004) Genes Dev. 18, 1263-1271
- 51. Okada, Y., Jiang, Q., Lemieux, M., Jeannotte, L., Su, L., and Zhang, Y. (2006) Nat. Cell Biol. 8, 1017-1024
- 52. Zeisig, B. B., Schreiner, S., Garcia-Cuellar, M. P., and Slany, R. K. (2003) Leukemia 17, 359 – 365
- 53. Carlson, M. (1997) Annu. Rev. Cell Dev. Biol. 13, 1-23
- 54. Andrau, J. C., van de Pasch, L., Lijnzaad, P., Bijma, T., Koerkamp, M. G., van de Peppel, J., Werner, M., and Holstege, F. C. (2006) Mol. Cell 22,
- 55. Zhu, X., Wiren, M., Sinha, I., Rasmussen, N. N., Linder, T., Holmberg, S., Ekwall, K., and Gustafsson, C. M. (2006) Mol. Cell 22, 169-178
- 56. Hallberg, M., Polozkov, G. V., Hu, G. Z., Beve, J., Gustafsson, C. M., Ronne, H., and Bjorklund, S. (2004) Proc. Natl. Acad. Sci. U. S. A. 101, 3370 – 3375
- 57. Gu, W., Malik, S., Ito, M., Yuan, C. X., Fondell, J. D., Zhang, X., Martinez, E., Qin, J., and Roeder, R. G. (1999) Mol. Cell 3, 97-108
- 58. Mo, X., Kowenz-Leutz, E., Xu, H., and Leutz, A. (2004) Mol. Cell 13, 241 - 250
- 59. Akoulitchev, S., Chuikov, S., and Reinberg, D. (2000) Nature 407, 102-106
- 60. Wang, G., Balamotis, M. A., Stevens, J. L., Yamaguchi, Y., Handa, H., and Berk, A. J. (2005) Mol. Cell 17, 683-694
- 61. Elmlund, H., Baraznenok, V., Lindahl, M., Samuelsen, C. O., Koeck, P. J., Holmberg, S., Hebert, H., and Gustafsson, C. M. (2006) Proc. Natl. Acad. Sci. U. S. A. 103, 15788-15793
- 62. Pavri, R., Lewis, B., Kim, T. K., Dilworth, F. J., Erdjument-Bromage, H., Tempst, P., de Murcia, G., Evans, R., Chambon, P., and Reinberg, D. (2005) Mol. Cell 18, 83-96
- 63. Malik, S., Baek, H. J., Wu, W., and Roeder, R. G. (2005) Mol. Cell Biol. 25, 2117-2129
- 64. Ryu, S., and Tjian, R. (1999) Proc. Natl. Acad. Sci. U. S. A. 96, 7137-7142
- 65. Taatjes, D. J., Marr, M. T., and Tjian, R. (2004) Nat. Rev Mol. Cell. Biol. 5, 403 - 410



# Induction CMV HeLa Cell Line

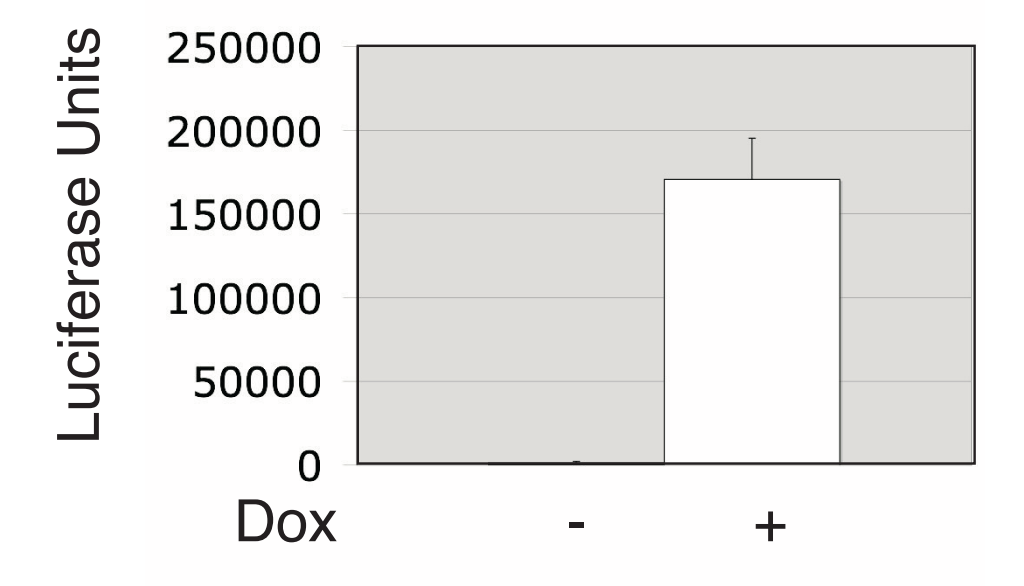


Fig. S1: Luciferase induction in a HeLa cell line carrying a stable plasmid (pML53) under the control of the bidirectional tetO CMV promoters. A representative experiment showing 170-fold induction is depicted. Doxycyline (1  $\mu$ g/ml) was added for 24 hours prior to measurement of luciferase activity.

Figure S1

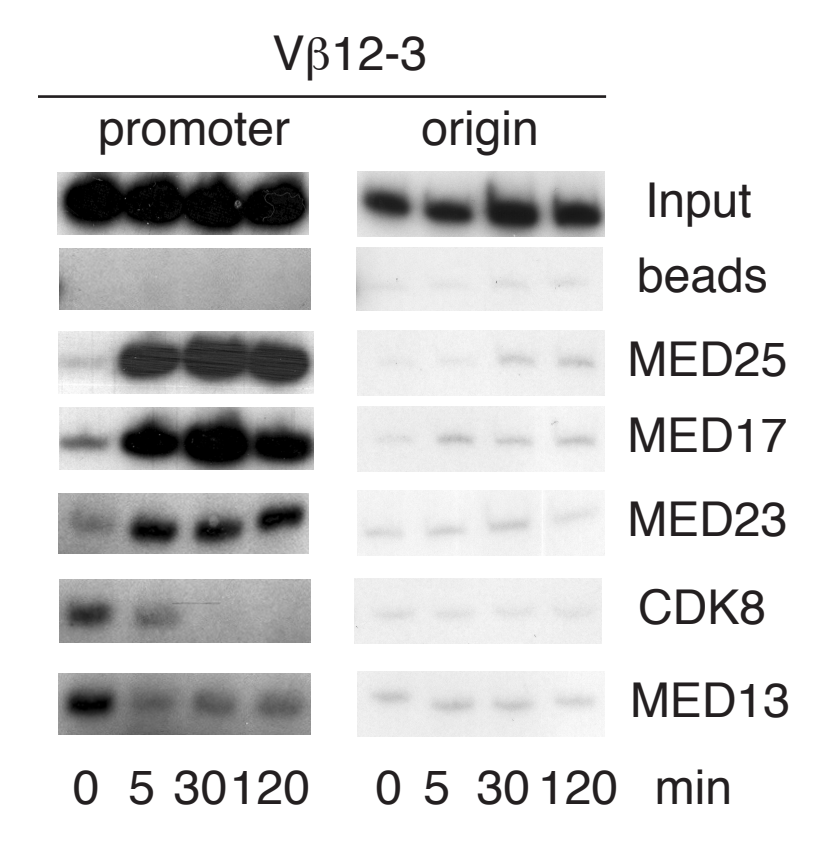


Fig. S2. Kinetics of Mediator recruitment to  $V\beta12-3$  and ori control regions. In this independent analysis Mediator is not detected at the origin of replication.

## The VP16 Activation Domain Establishes an Active Mediator Lacking CDK8 in Vivo

Thomas Uhlmann, Stefan Boeing, Michael Lehmbacher and Michael Meisterernst

J. Biol. Chem. 2007, 282:2163-2173.

doi: 10.1074/jbc.M608451200 originally published online November 29, 2006

Access the most updated version of this article at doi: 10.1074/jbc.M608451200

#### Alerts:

- When this article is cited
- · When a correction for this article is posted

Click here to choose from all of JBC's e-mail alerts

## Supplemental material:

http://www.jbc.org/content/suppl/2006/12/06/M608451200.DC1.html

This article cites 65 references, 23 of which can be accessed free at http://www.jbc.org/content/282/4/2163.full.html#ref-list-1